Articles

Chinese Science Bulletin

Geophysics

March 2010 Vol.55 No.8: 718−722
doi: 10.1007/s11434-009-0538-z

Electron density hole and quadruple structure of B_y during collisionless magnetic reconnection

HUANG Can[1,2], WANG RongSheng[1], LU QuanMing[1,2*] & WANG Shui[1]

[1] *CAS Key Laboratory of Basic Plasma Physics, School of Earth and Space Sciences, University of Science and Technology of China, Hefei 230026, China;*
[2] *Key Laboratory for Space Weather, Chinese Academy of Sciences, Beijing 100190, China*

Received April 7, 2009; accepted June 24, 2009; published online November 3, 2009

In collisionless reconnection, the magnetic field near the separatrix is stronger than that around the X-line, so an electron-beam can be formed and flows toward the X-line, which leads to a decrease of the electron density near the separatrix. Having been accelerated around the X-line, the electrons flow out along the magnetic field lines in the inner side of the separatrix. A quadruple structure of the Hall magnetic field B_y is formed by such a current system. A 2D particle-in-cell (PIC) simulation code is used in this paper to study the collisionless magnetic reconnection without an initial guide field. The current system described above is proved by the simulations. Furthermore, the position of the peak of the Hall magnetic field B_y is found to be between the separatrix and the center of the current sheet, which is verified by Cluster observations.

collisionless magnetic reconnection, electron density hole, quadruple structure

Citation: Huang C, Wang R S, Lu Q M, et al. Electron density hole and quadruple structure of B_y during collisionless magnetic reconnection. Chinese Sci Bull, 2010, 55: 718−722, doi: 10.1007/s11434-009-0538-z

Magnetic reconnection provides a physical mechanism for fast energy conversion from magnetic energy to kinetic energy of plasma, which is used to explain many bursts in solar atmosphere, interplanetary space and the Earth's magnetosphere [1,2]. Considering negligible collisions between particles in these environments, it is generally assumed that space plasma is collisionless. Recent researches show that the Hall effect plays an important role in collisionless magnetic reconnection [3,4].

In collisionless reconnection, the reconnection region can be divided into several subregions. At scale lengths of c/ω_{pi} (where c/ω_{pi} is the ion inertial length), both ions and electrons are frozen-in, where Alfven waves dominate. At scale lengths below c/ω_{pi}, only the electrons are frozen-in, and whistler waves work. The frozen-in constraint of electrons is finally broken when the scale sizes in the system approaches c/ω_{pe} (where c/ω_{pe} is the electron inertial length) [5−7]. During Hall magnetic reconnection, the magnetic field near the separatrix is much stronger than that around the X-line, which leads to an electron beam formed and flowing into the X-line along the separatrix. These electrons flow out along the magnetic field lines in the inner side of the current sheet after the acceleration around the X-line. A quadruple structure of the Hall magnetic field B_y is formed by such a current system [8,9]. It is found by scientific observation that there are electron density holes near the separatrix [5,10]. With Hall-MHD simulation, Yang et al. [11] found that the plasma density around the X-line is low. A 2D particle-in-cell (PIC) simulation code is used to study the relationship between the position of the peak of B_y and the cavity of the electron density during collisionless magnetic reconnection without an initial guide field. Furthermore, some observations of Cluster are used to prove the numerical results.

1 Model

A 2D PIC simulation code [12] is used in this paper to in-

*Corresponding author (email: qmlu@ustc.edu.cn)

© Science China Press and Springer-Verlag Berlin Heidelberg 2009

vestigate the electron dynamics in magnetic reconnection. In the simulation, the electromagnetic fields are defined on the grids and are updated by solving the Maxwell equations with a full explicit algorithm. In our simulation model, the initial configuration is a 1D Harris current sheet in the (x, z) plane, and the initial magnetic field is given by

$$\boldsymbol{B}_0(z) = B_0 \tanh\left[\left(z-\frac{L_z}{2}\right)\Big/\delta\right]\mathbf{e}_x,$$

where δ is the half-width of the current sheet, $\boldsymbol{B}_0$ is the asymptotical magnetic strength, L_z is the size of the simulation domain in the z direction. The corresponding number-density is

$$n(z) = n_b + n_0 \operatorname{sech}^2\left[\left(z-\frac{L_z}{2}\right)\Big/\delta\right],$$

where n_b represents the density of the background plasma and n_0 is the peak Harris density. The plasma particle distribution functions for the ions and electrons are Maxwellian, and their drift speeds in the y direction satisfy $V_{i0}/V_{e0}=T_{i0}/T_{e0}$, where $V_{i0}(V_{e0})$ and $T_{i0}(T_{e0})$ are the drift speed and initial temperature for ions(electrons), respectively. In our simulations, the temperature ratio is $T_{i0}/T_{e0}=5$, and $n_0=5n_b$. The current sheet width is $\delta=0.5\ c/\omega_{pi}$, where c/ω_{pi} is the ion inertial length defined by n_0. Current researches show that the change of the mass ratio does not make much difference to the reconnection rate [13], so the mass ratio is set to $m_i/m_e=100$. The light speed is set to $c=15v_A$ (it is generally thought that the change of c/v_A has little effect on the evolvement of the system [14]), where v_A is the Alfven speed defined by B_0 and n_0.

The computation is carried out in a rectangular domain in the (x, z) plane with dimension $L_x\times L_z=(25.6\ c/\omega_{pi})\times(12.8\ c/\omega_{pi})$. An $N_x\times N_z=512\times256$ grid system is employed, so the spatial resolution is $\Delta x=\Delta z=0.05\ c/\omega_{pi}=0.5\ c/\omega_{pe}$. The time step is $\Omega_i\Delta t=0.001$. We employ more than 1.0×10^7 particles per species. The periodic boundary conditions are used along the x direction, while the ideal conducting boundary conditions for electromagnetic fields are employed in the y direction. In order to make the system enter the nonlinear stage quickly, an initial flux perturbation is introduced as follows, which is useful to research the stage of rapid growth of reconnection rate.

$$\psi(x,z) = -\psi_0 \cos\left[2\pi\left(x-\frac{L_x}{2}\right)\Big/L_x\right]\cos\left[2\pi\left(z-\frac{L_z}{2}\right)\Big/L_z\right].$$

The corresponding magnetic field perturbation is

$$\boldsymbol{B} = -2\pi\psi_0/L_z\cdot\cos\left[2\pi\left(x-\frac{L_x}{2}\right)\Big/L_x\right]\sin\left[2\pi\left(z-\frac{L_z}{2}\right)\Big/L_z\right]\mathbf{e}_x$$
$$+2\pi\psi_0/L_x\cdot\sin\left[2\pi\left(x-\frac{L_x}{2}\right)\Big/L_x\right]\cos\left[2\pi\left(z-\frac{L_z}{2}\right)\Big/L_z\right]\mathbf{e}_z,$$

where Ψ is the y component of the vector potential, and Ψ_0 is set to $\Psi_0/(B_0c/\omega_{pi})=0.05$.

2 Results

The configuration evolution of magnetic fields in (x, z) plane is presented in Figure 1, which shows the stage of start, rapid connection rate growth and saturation. In the process of reconnection, the magnetic field lines approach the center of the simulation region, then, they are broken and reconnected again. The magnetic lines are so bent that the flux flows out from the flank of the separatrix under the magnetic pressure. Afterward, more and more magnetic lines take part in this process. At $\Omega_it=18$, an obvious X-line is formed, when the half-width of the island is about 1.0 c/ω_{pi}. The half-width of the island is about 2.0 c/ω_{pi} and the reconnection rate reaches the maximum at $\Omega_it=23$. At $\Omega_it=28$, reconnection is stopped and the half-width of the island reaches about 2.8 c/ω_{pi}.

Figure 2 shows the ion and electron velocity distribution, the quadruple structure of B_y/B_0, and the electron density $\log(n/n_0)$ at $\Omega_it=23$. In the figure, the background contour lines are the magnetic field lines in (x, z) plane and the pecked lines are the separatrixes. Figure 2(a) shows that the macroscopical dynamics effect of ions is important only in the inflow region and outflow region—ions flow from the flank of the current sheet into the center and flow out in the outflow region with the maximum velocity 0.6 v_A. In other words, ions flow into the center of the current sheet carrying flux, and the magnetic energy is converted into kinetic energy of plasma near the X-line. So it lies on the behaviors ions to change the magnetic topology. The ion dynamics is negligible at the X-line, around the separatrix or in the quadruple structure region, where the macroscopical flow of electrons is obvious. In Figure 2(b), there is an electron beam along the separatrix, which results from the magnetic mirror effect. Besides, due to the electric field in the y di-

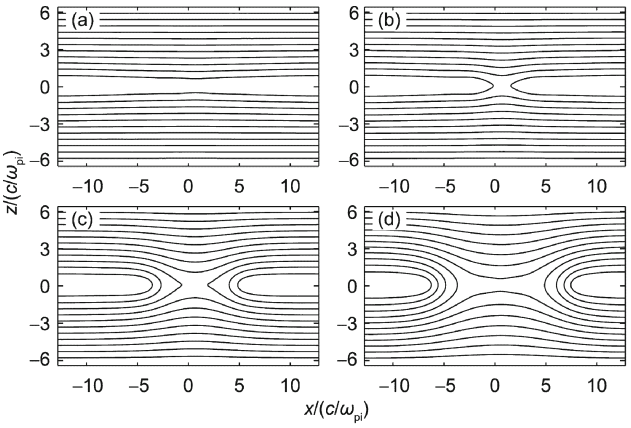

Figure 1 The configurations of magnetic field lines in (x,z) plane at (a) $\Omega_it=13$, (b) $\Omega_it=18$, (c) $\Omega_it=23$, (d) $\Omega_it=28$.

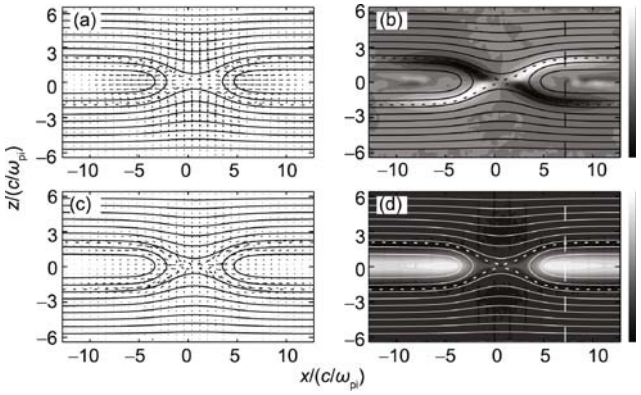

Figure 2 Several physical quantities at $\Omega_i t$ =23: (a) the velocity field of ions; (b) the velocity field of electrons; (c) the quadruple structure of B_y/B_0; (d) the density of electron $\log(n/n_0)$.

rection, electrons drift to the X-line. There is another electron beam, which is 0.2–0.5 c/ω_{pi} far away from the inner-side of the separatrix, flowing out from the X-line with the maximum velocity $2.8v_A$ after the acceleration around the X-line [15]. These flows of ions and electrons form a current system-the current flows into the X-line along the inner side of the separatrix and flows out along the separatrix. Conceivably, a quadruple structure of B_y as shown in Figure 2(c) is formed by such a current system. Furthermore, there is a long and narrow electron density hole around the separatrix, which is in the same region of the electron beam flowing into the X-line. Right above or below the X-line, there is another electron density hole because of the electrostatic drift.

Following the above, it is easy to understand that the position of the peak of B_y is at the inner side of the separatrix. Figure 3 shows the profile of B_y and the density of electron along the line of $x(c/\omega_{pi})$=7.2 (the dash lines in Figure 2(c) or 2(d)). The real line and the dash line show the n/n_0 and B_y/B_0, respectively. The dot lines marked with A and B show the position of the peak of B_y/B_0 and the valley of n/n_0, respectively. It is apparent that the position of the peak of B_y is closer to current sheet than to the separatrix. The peak of B_y

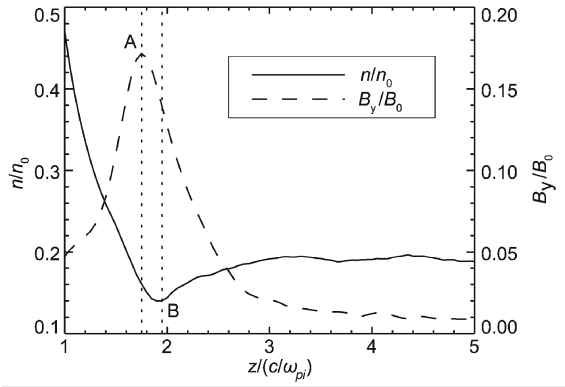

Figure 3 The profile of B_y and the density of electron along the line of $x(c/\omega_{pi})$=7.2.

can be estimated by the equation $\boldsymbol{j}=\frac{1}{\mu_0}\nabla\times\boldsymbol{B}$. A pair of antiparallel current sheets are considered for the estimation, from which we can get $B_y=\mu_0 rj$ (where r is the half-distance between the two current sheets, and it is assumed to be 0.1 c/ω_{pi}. j is the sum of the absolute value of the two current sheets). According to the equation $\boldsymbol{j}=n_i e\boldsymbol{u}_i-n_e e\boldsymbol{u}_e \approx -n_e e\boldsymbol{u}_e$ (where n and $\boldsymbol{u}$ represent the number density and field velocity, respectively; the subscripts $\boldsymbol{j}$ and $\boldsymbol{e}$ identify ions and electroms), we can get $B_y \approx \mu_0 r n_e e\boldsymbol{u}_e$. If $\boldsymbol{j}=n_i e\boldsymbol{u}_i-n_e e\boldsymbol{u}_e \approx -n_e e\boldsymbol{u}_e$, the peak of B_y is about $0.2B_0$.

3 Conclusions and discussion

A 2D PIC simulation code is used in this paper to study the collisionless magnetic reconnection without an initial guide field. The results show that the ion behaviors determine the topological structure of magnetic field. The magnetic field near the separatrix is much stronger than that around the X-line, which causes to form an electron beam flowing into X-line along the separatrix and to deplete the density of electron near the separatrix. There is another electron beam along the inner side of the separatrix, which flows out after the acceleration around the X-line. A quadruple structure of the Hall magnetic field B_y is formed by such a current system. Furthermore, the position of the peak of B_y is closer to current sheet than to the separatrix (the electron density hole). The Hall-MHD's results also show that the position of the peak of B_y is closer to current sheet than to the valley of plasma density [11].

The Cluster consists of four identical satellites (C1, C2, C3 and C4) and was successfully launched in 2000. A typical reconnection event is detected between 07:50 UT and 08:05 UT on Sept. 10, 2001 when Cluster stays around 19 R_E (R_E, the Earth radii) in the magnetotail. Figure 4 shows the data of magnetic field and plasma. The first panel shows the electron density obtained from the spacecraft potential measurements of the EFW [16,17] instrument, the time resolution of which is 1/5 s. The following three panels denote the three components of magnetic field from the FGM [18] instrument. The last panel shows the x component of the high speed flow from CIS [19] instrument. The Geocentric Solar Magnetospheric (GSM) coordinates system is used throughout this part. During 07:52−08:02 UT, the Cluster detects a tailward high speed flow followed by an earthward high speed flow. Simultaneously, the z component of the magnetic field (B_z) reverses from south to north. During the tailward high speed flow, the x component of magnetic field (B_x) measured by C3 (C1, C2 and C4) remains mostly negative (positive), which means that C3 (C1, C2 and C4) stays predominantly in the southward (northward) side of the current sheet. When in the earthward high

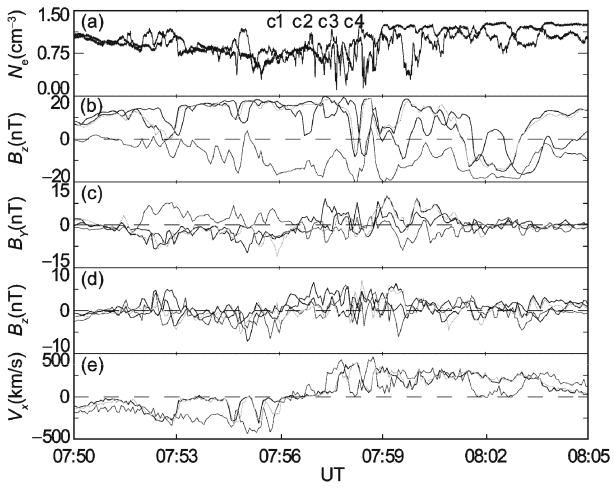

Figure 4 (a) The electron density, (b)–(d) the three components of magnetic field, (e) the *x* component of the high-speed flow for spacecraft 1 to 4, respectively.

speed flow, C3 (C1, C2 and C4) observes positive (negative) values of B_y. However, when the Cluster enters the earthward of the X-line, C3 (C1, C2 and C4) observes mainly negative (positive) values of B_y. This is in agreement with the quadrupolar out-of-plane Hall magnetic field configuration. The coincidence of the V_x and B_z reversals and clear Hallquadrupolar magnetic field indicate that Cluster crosses an active reconnection diffusion region from the tailward side to the earthward side [20]. During the crossing, C1 and C2 encounter the electron cavity (the electron density decreases by 40%) several times. Figure 5 shows the data of the high time resolution from the C2 satellite between 07:54:35 UT and 07:55:35 UT. The top panel shows the electron density. The other three panels denote the three components of magnetic field. The solid and dashed vertical lines denote the maximum value of B_y and the minimum value of the electron density, respectively. We can see that the minimum value of the electron density appears when B_x is about 18 nT. The peaks of B_x is located where B_x is about 10—15 nT. So the electron density cavity is located above the position of the peak of B_y. In the period from 07:52 UT to 08:02 UT, Cluster crosses the electron cavity several times. We analyze other crossings and find that the results are consistent with the measurement from C2.

The observations above are consistent with the simulation results, which verify our descriptions of the electron flow: the electrons flow to the X-line along the separatrix, and then they flow out from the X-line along the magnetic field lines at the inner side of the separatrix after the acceleration around the X-line.

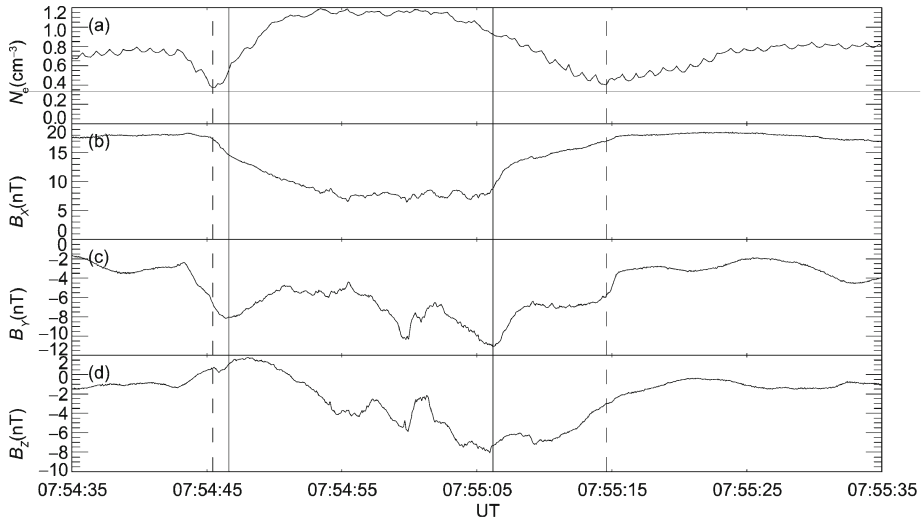

Figure 5 (a) The electron density, (b)–(d) the three components of magnetic field, (e) the *x* component of the high-speed flow taken from C2.

The authors would like to thank the group FGM, ICS and EFW of Cluster. This work was supported by the Knowledge Innovation Project of Chinese Academy of Sciences (*Grant No. KJCX2-YW-N28*)*, National Natural Science Foundation of China* (*Grant Nos. 40674093, 40725013 and 40874075*) *and Specialized Research Fund for State Key Laboratories.*

1 Biskamp D. Magnetic Reconnection in Plasma. Cambridge: Cambridge University Press, 2000
2 Priest E, Forbes T. Magnetic Reconnection: MHD Theory and Applications. Cambridge: Cambridge University Press, 2000
3 Wang S, Lee L C. Magnetic Reconnection (in Chinese). Hefei: Anhui Education Press, 1999
4 Wang X, Bhattacharjee A, Ma Z W. Scaling of collisionless forced reconnection. Phys Rev Lett, 2001, 87: 265003
5 Øieroset M, Phan T D, Fujimoto M, et al. *In situ* detection of collisionless reconnection in the Earth's magnetotail. Nature, 2001, 412: 414–417
6 Birn J. Geospace environmental modeling (GEM) magnetic reconnection challenge. J Geophys Res, 2001, 106: 3715–3719
7 Shay M A, Drake J F, Rogers B N, et al. Alfvénic collisionless reconnection and the Hall term. J Geophys Res, 2001, 106: 3754
8 Pritchett P L. Geospace environment modeling magnetic reconnection challenge: Simulations with a full particle electromagnetic code. J Geophys Res, 2001, 108: 3783

9 Nagai T, Shinohara I, Fujimoto M, et al. Structure of the Hall current system in the vicinity of the magnetic recoonection site. J Geophys Res, 2003, 108: 1357
10 Mozer F S, Bale S D, Phan T D. Evidence of diffusion regions at a subsolar magnetopause crossing. Phys Rev Lett, 2003, 89: 015002
11 Yang H A, Jin S P, Zhou G C. Density depletion and Hall effect in magnetic reconnection. J Geophys Res, 2006, 111: A11223
12 Lu Q M, Cai D S. Implementation of parallel plasma particle-in-cell codes on PC cluster. Comput Phys Commun, 2001, 139: 93–104
13 Guo J, Lu Q M. Effects of ion-electron mass ratio on electron dynamics in collisionless magnetic reconnection. Chin Phys Lett, 2007, 24: 3199
14 Birdsall C K, Longdon A B. Plasma Physics via Computer Simulation. New York: McGraw-Hill Book Company, 1991
15 Fu X R, Lu Q M, Wang S. The process of electron acceleration during collisionless magnetic reconnection. Phys Plasmas, 2006, 13: 012309
16 Balogh A. The Cluster magnetic field investigation: overview of in-flight performance and initial results. Ann Geophys, 2001, 19: 1207–1217
17 Gustafsson G. First results of electric field and density observations by Cluster EFW based on initial months of operation. Ann Geophys, 2001, 19: 1219–1240
18 Pedersen A. Electron density estimations derived from spacecraft potential measurements on Cluster in tenuous plasma regions. J Geophys Res, 2008, 113: A07S33
19 Rème H. First multispacecraft ion measurements in and near the Earth's magnetosphere with the identical Cluster ion spectrometry(CIS)experiment. Ann Geophys, 2001, 19: 1303
20 Wang R S, Lu Q M, Guo J, et al. Spatial distribution of energetic electrons during magnetic reconnection. Chin Phys Lett, 2008, 25: 3083–3085